Available online at www.sciencedirect.com
ScienceDirect
Journal of Sound and Vibration 297 (2006) 794–809
JOURNAL OF SOUND AND VIBRATION
www.elsevier.com/locate/jsvi

Dynamic responses of the in-plane and out-of-plane vibrations for an axially moving membrane

Changho Shin[a], Jintai Chung[b,*], Hong Hee Yoo[c]

[a]*Department of Precision Mechanical Engineering, Graduate School, Hanyang University, 17 Haengdang-dong, Seongdong-gu, Seoul 133-791, Republic of Korea*
[b]*Department of Mechanical Engineering, Hanyang University, 1271 Sa-1-dong, Ansan, Kyunggi-do 425-791, Republic of Korea*
[c]*School of Mechanical Engineering, Hanyang University, 17 Haengdang-Dong Sungdong-Gu, Seoul 133-791, Republic of Korea*

Received 5 January 2005; received in revised form 21 February 2006; accepted 24 April 2006
Available online 7 July 2006

Abstract

The dynamic responses of both the in-plane and out-of-plane vibrations are investigated for an axially moving membrane. Using the extended Hamilton principle, equations of motion are derived for the moving membrane with no-slip boundary conditions at rollers. The equations of motion are discretized by using the Galerkin method and then the generalized-α time integration method is applied to compute the dynamic responses of the membrane. Based on the computed results, the responses are compared between the in-plane and out-of-plane vibrations. In addition, the effects of translating velocity/acceleration, critical speeds and velocity profiles on the dynamic behaviours for displacements and stresses are investigated and discussed.
© 2006 Elsevier Ltd. All rights reserved.

1. Introduction

Axially moving membranes have many engineering applications, for instance, paper production, printing processes, web transport systems and tape recording. In these applications, the vibration levels and transporting speeds of membranes are major concerns. A severe vibration level of a membrane does not only result in breaks during production of paper or web, but it also leads to poor quality in printing or recording processes. Since the natural frequencies of a membrane decreases with the transporting speed and eventually the membrane may encounter instability, there is a limitation on increasing the transporting speed. The limitation in the speed restricts high productivity in manufacturing.

A vast amount of research has been performed on axially moving materials such as moving strings, beams and plates. Many important studies on the stability [1–4], modal analysis [1,2,5,6], discretization [5,7], and nonlinear vibration [8–10] of the moving materials were reported. In addition, the effects of unsteady gyroscopic systems [11,12] and parametric excitation [13–15] on the moving materials were also investigated. However, not many studies related to axially moving membranes have been presented. Some research works

*Corresponding author. Tel.: +82 31 400 5287; fax: +82 31 406 5550.
E-mail address: jchung@hanyang.ac.kr (J. Chung).

0022-460X/$ - see front matter © 2006 Elsevier Ltd. All rights reserved.
doi:10.1016/j.jsv.2006.04.031

on the moving membrane are follows. The longitudinal vibration of a moving magnetic tape was studied by Wickert [16], who found that in a particular transport speed range longitudinal motion of the tape can be self-excited through negative damping for small amplitude vibration and positive damping for large amplitudes. Shin et al. [17] studied the free in-plane vibration of an axially moving membrane considering the effects of the translating speed and aspect ratio of the membrane. Their study showed that translating speed, aspect ratio, and boundary conditions have significant effects on the in-plane vibrations of the moving membrane. Different from the above studies on the in-plane vibrations, Koivurova and Pramila [18] analysed the out-of-plane or transverse vibration of a moving membrane by using the finite-element method. In their study, it was found that nonlinearities and coupling phenomena have a considerable effect on the dynamic behaviour of the system. As an extended study for Ref. [18], the transverse vibrations of an axially moving membrane submerged in ideal fluid were investigated by Niemi and Pramila [19]. On the other hand, Wang [20] analysed the vibration of an axially moving web, controlled through self-acting air bearings. He pointed out that the pressurized air layers between a moving web and bearing surfaces can significantly reduce the transverse web deflection and provide a means of effective stabilizing. Even though many studies on axially moving membranes have been presented, to the authors' knowledge, there is no study on an axially moving membrane which considers both the in-plane and out-of-plane vibrations simultaneously.

In this paper, the dynamic responses of an axially moving membrane are investigated. Using the extended Hamilton principle [21], nonlinear coupled equations of motion are derived for both the in-plane and out-of-plane displacements. During the derivation, the translating acceleration and geometric nonlinearity of the membrane are considered. The derived equations are discretized by using the Galerkin approximation method, and then the nonlinear dynamic responses are computed by using the generalized-α time integration method [22] without a nonlinear equation solver. From the computed dynamic responses, the effects of the translating velocity and acceleration on the dynamic behaviours are analysed. In addition, deformed shapes and stress distributions are also investigated.

2. Equations of motion

Fig. 1 shows the model of a membrane moving in the x direction with translating velocity V and acceleration $\dot{V}$. The moving membrane with width b and thickness h is supported by two pairs of rollers separated by distance L. The right rollers are driving rollers and the left rollers are driven ones. When the membrane is accelerated or decelerated, the tension at the right end is different from the tension at the left end. Denoting the tensions per unit width at the right and left ends by T_L and T_0, respectively, the tension T_L can be expressed in terms of T_0 and $\dot{V}$:

$$T_L = T_0 + \rho h L \dot{V} \tag{1}$$

where ρ is the mass density of the membrane. In addition to the tensions, the membrane is subjected to pressure p in the z direction.

The membrane may have deformation as well as rigid-body motion. The rigid-body motion is described by the translating velocity and acceleration. When point P moves to point P' by only the deformation of the membrane, the displacement of point P can be represented by displacements in the x, y and z directions.

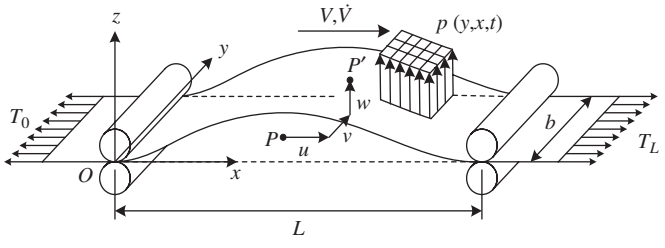

Fig. 1. Configuration of an axially moving membrane with translating velocity V and acceleration $\dot{V}$.

These displacements are denoted by u, v and w, which are known as the longitudinal, lateral and transverse displacements, respectively. Because u and v are in the plane of the undeformed membrane, they are called the in-plane displacements. However, w is perpendicular to the membrane, so it is called the out-of-plane displacement. Since u, v and w are functions of time t as well as the x and y coordinates, they can be represented by

$$u = u(t, x, y), \quad v = v(t, x, y), \quad w = w(t, x, y). \tag{2}$$

The equations of motion can be derived by using the extended Hamilton principle [21]:

$$\int_{t_1}^{t_2} (\delta K - \delta U + \delta W_{\text{nc}} - \delta M)\, \mathrm{d}t = 0, \tag{3}$$

where t_1 and t_2 are arbitrary time, δ is the variation operator, K is the kinetic energy, U is the potential energy, W_{nc} is work done by the non-conservative force, and M is the momentum transport across the boundaries.

The variation of kinetic energy for the moving membrane can be written by

$$\delta K = \rho h \int_A \mathbf{v} \cdot \delta \mathbf{v}\, \mathrm{d}A, \tag{4}$$

where A is the area of the membrane i.e., $A = bL$ and $\mathbf{v}$ is the velocity vector given by

$$\mathbf{v} = \left(V + \frac{\partial u}{\partial t} + V\frac{\partial u}{\partial x}\right)\mathbf{i} + \left(\frac{\partial v}{\partial t} + V\frac{\partial v}{\partial x}\right)\mathbf{j} + \left(\frac{\partial w}{\partial t} + V\frac{\partial w}{\partial x}\right)\mathbf{k}, \tag{5}$$

in which $\mathbf{i}$, $\mathbf{j}$ and $\mathbf{k}$ are unit vectors in the x, y and z directions, respectively. On the other hand, the variation of potential energy may be given by

$$\delta U = \int_A (q_x \delta\varepsilon_x + q_y \delta\varepsilon_y + 2q_{xy}\delta\varepsilon_{xy})\, \mathrm{d}A, \tag{6}$$

where q_x, q_y and q_{xy} are the linearized membrane forces per unit length while ε_x, ε_y and ε_{xy} are the nonlinear strains. These stresses and strains are functions of the displacements u, v and w:

$$q_x = \frac{Eh}{1-v^2}\left(\frac{\partial u}{\partial x} + v\frac{\partial v}{\partial y}\right), \quad q_y = \frac{Eh}{1-v^2}\left(\frac{\partial v}{\partial y} + v\frac{\partial u}{\partial x}\right), \quad q_{xy} = \frac{Eh}{2(1+v)}\left(\frac{\partial u}{\partial y} + \frac{\partial v}{\partial x}\right), \tag{7}$$

$$\varepsilon_x = \frac{\partial u}{\partial x} + \frac{1}{2}\left(\frac{\partial w}{\partial x}\right)^2, \quad \varepsilon_y = \frac{\partial v}{\partial y} + \frac{1}{2}\left(\frac{\partial w}{\partial y}\right)^2, \quad \varepsilon_{xy} = \frac{1}{2}\left(\frac{\partial u}{\partial y} + \frac{\partial v}{\partial x} + \frac{\partial w}{\partial x}\frac{\partial w}{\partial y}\right), \tag{8}$$

in which E is Young's modulus and v is Poisson's ratio. Note that Eq. (8) represent the von Karman strain theory which demonstrates the geometrically nonlinear relations between the strains and displacements. Although linear stresses are used for modelling, the dynamic behaviour of the membrane can be well described by the geometric nonlinearity caused by large deformation.

Assuming that the pressure p is exerted over the entire membrane surface, the virtual work done by non-conservative forces is given by

$$\delta W_{\text{nc}} = \int_0^b (T_L\, \delta u|_{x=L} - T_0\, \delta u|_{x=0})\, \mathrm{d}y + \int_A p\, \delta w\, \mathrm{d}A. \tag{9}$$

On the other hand, the variation of the momentum transport can be expressed as

$$\delta M = \rho h V \int_0^b \mathbf{v} \cdot \delta \mathbf{r}|_{x=0}^{L}\, \mathrm{d}y \tag{10}$$

where $\mathbf{r}$ is the displacement vector given by

$$\mathbf{r} = (x+u)\mathbf{i} + (y+v)\mathbf{j} + w\mathbf{k}. \tag{11}$$

The introduction of Eqs. (4), (6), (9) and (10) into Eq. (3) yields the following equations of motion:

$$\rho h\left(\frac{\partial^2 u}{\partial t^2}+2V\frac{\partial^2 u}{\partial t\,\partial x}+V^2\frac{\partial^2 u}{\partial x^2}+\dot{V}\frac{\partial u}{\partial x}\right)-\frac{\partial q_x}{\partial x}-\frac{\partial q_{xy}}{\partial y}=-\rho h\dot{V}, \tag{12}$$

$$\rho h\left(\frac{\partial^2 v}{\partial t^2}+2V\frac{\partial^2 v}{\partial t\,\partial x}+V^2\frac{\partial^2 v}{\partial x^2}+\dot{V}\frac{\partial v}{\partial x}\right)-\frac{\partial q_y}{\partial y}-\frac{\partial q_{xy}}{\partial x}=0, \tag{13}$$

$$\rho h\left(\frac{\partial^2 w}{\partial t^2}+2V\frac{\partial^2 w}{\partial t\,\partial x}+V^2\frac{\partial^2 w}{\partial x^2}+\dot{V}\frac{\partial w}{\partial x}\right)-\frac{\partial}{\partial x}\left(q_x\frac{\partial w}{\partial x}+q_{xy}\frac{\partial w}{\partial y}\right)-\frac{\partial}{\partial y}\left(q_y\frac{\partial w}{\partial y}+q_{xy}\frac{\partial w}{\partial x}\right)=p. \tag{14}$$

Note that Eqs. (12) and (13) describe the in-plane motion of the membrane while Eq. (14) describes the out-of-plane motion. Since q_x, q_y and q_{xy} can be expressed in terms of u and v, Eqs. (12) and (13) are partial differential equations coupled through only the in-plane displacements. This means equations (12) and (13) can be solved without considering the out-of-plane displacement w. It should be noted that the in-plane and out-of-plane displacements are in Eq. (14). Furthermore, this equation is a nonlinear partial differential equation because the membrane forces are functions of the in-plane displacements. The appearance of the in-plane displacements in the equation of out-of-plane motion implies that that the transverse vibration is influenced by the membrane forces.

Next, consider the boundary conditions for the axially moving membrane. Even though the membrane can have various cases of boundary conditions at the rollers, this paper deals with only no slipping boundary conditions. When there is no slipping between the membrane and the rollers in the y direction, the boundary conditions at the right and left ends are given by

$$q_x=T_0,\quad v=w=0\quad\text{at}\quad x=0, \tag{15}$$

$$q_x=T_L,\quad v=w=0\quad\text{at}\quad x=L. \tag{16}$$

Since the sides corresponding to $y=0$ and $y=b$ have no traction, the boundary condition at these sides may be given by

$$q_y=q_{xy}=q_y\frac{\partial w}{\partial y}+q_{xy}\frac{\partial w}{\partial x}=0\quad\text{at}\quad y=0,\ b. \tag{17}$$

3. Discretization of the equations of motion

By using the Galerkin method, approximate solutions are obtained from the partial differential equations of Eqs. (12)–(14) with the boundary conditions of Eqs. (15)–(17). Since it is difficult to find the comparison functions for this problem, the equations of motion are transformed into the weak forms that require the admissible functions instead of the comparison functions. Two weak forms are derived in this paper: one is for the in-plane motion and the other is for the out-of-plane motion. As pointed out in the previous section, since the equations of in-plane motion are coupled through only the in-plane displacements, these equations can be solved independently of the out-of-plane displacement. Moreover, once the in-plane displacements are determined, the equations of out-of-plane motion may be regarded as a linear partial differential equation because the membrane forces q_x, q_y and q_{xy} become prescribed known functions.

For these reasons, it is convenient for analysis to derive two weak forms for the in-plane and out-of-plane motions. The derived weak form for the in-plane motion can be expressed as

$$\int_0^b\int_0^L\left[\rho h\bar{\mathbf{u}}^T\left(\frac{\partial^2\mathbf{u}}{\partial t^2}+2V\frac{\partial^2\mathbf{u}}{\partial t\,\partial x}+V^2\frac{\partial^2\mathbf{u}}{\partial x^2}+\dot{V}\frac{\partial\mathbf{u}}{\partial x}\right)+\bar{\boldsymbol{\varepsilon}}^T\mathrm{D}\boldsymbol{\varepsilon}\right]\mathrm{d}x\,\mathrm{d}y$$
$$=\int_0^b(T_L\bar{u}|_{x=L}-T_0\bar{u}|_{x=0})\mathrm{d}y-\rho h\dot{V}\int_0^b\int_0^L\bar{u}\,\mathrm{d}x\,\mathrm{d}y, \tag{18}$$

where $\bar{u}$, $\bar{v}$ and $\bar{w}$ are the weighting functions of u, v and w, respectively, and

$$\mathbf{u} = \{u, v\}^{\mathrm{T}}, \quad \bar{\mathbf{u}} = \{\bar{u}, \bar{v}\}^{\mathrm{T}}, \quad \boldsymbol{\varepsilon} = \left\{\frac{\partial u}{\partial x}, \frac{\partial v}{\partial y}, \frac{\partial u}{\partial y} + \frac{\partial v}{\partial x}\right\}^{\mathrm{T}}, \quad \bar{\boldsymbol{\varepsilon}} = \left\{\frac{\partial \bar{u}}{\partial x}, \frac{\partial \bar{v}}{\partial y}, \frac{\partial \bar{u}}{\partial y} + \frac{\partial \bar{v}}{\partial x}\right\}^{\mathrm{T}},$$

$$\mathbf{D} = \frac{Eh}{1-\nu^2}\begin{bmatrix} 1 & \nu & 0 \\ \nu & 1 & 0 \\ 0 & 0 & (1-\nu)/2 \end{bmatrix}. \tag{19}$$

The weak form for the out-of-plane motion may be represented by

$$\int_0^b \int_0^L \left[\rho h \bar{w}\left(\frac{\partial^2 w}{\partial t^2} + 2V\frac{\partial^2 w}{\partial t\,\partial x} + V^2\frac{\partial^2 w}{\partial x^2} + \dot{V}\frac{\partial w}{\partial x}\right) + \bar{\boldsymbol{\theta}}^{\mathrm{T}}\mathbf{Q}\boldsymbol{\theta}\right] \mathrm{d}x\,\mathrm{d}y = \int_0^b \int_0^L \bar{w} p\,\mathrm{d}x\,\mathrm{d}y, \tag{20}$$

where

$$\boldsymbol{\theta} = \left\{\frac{\partial w}{\partial x}, \frac{\partial w}{\partial y}\right\}^{\mathrm{T}}, \quad \bar{\boldsymbol{\theta}} = \left\{\frac{\partial \bar{w}}{\partial x}, \frac{\partial \bar{w}}{\partial y}\right\}^{\mathrm{T}}, \quad \mathbf{Q} = \begin{bmatrix} q_x & q_{xy} \\ q_{xy} & q_y \end{bmatrix}. \tag{21}$$

Since the natural boundary conditions have already been applied during derivation of the weak forms, the admissible functions can be used as the basis functions for the displacements. Thus, the displacements of the membrane may be approximated as

$$u = \sum_{i=0}^{N_x}\sum_{j=0}^{N_y} T_{ij}^u(t) X_i(x) Y_j(y), \quad v = \sum_{i=0}^{N_x}\sum_{j=0}^{N_y} T_{ij}^v(t) Y_j(y)\,\sin(i+1)\pi x/L,$$

$$w = \sum_{i=0}^{M_x}\sum_{j=0}^{M_y} T_{ij}^w(t) Y_j(y)\sin(i+1)\pi x/L, \tag{22}$$

where N_x and N_y are the total numbers of the basis functions for the in-plane displacements in the x and y directions, respectively, M_x and M_y are the total numbers of the basis functions for the out-of-plane displacement, $T_{ij}^u(t)$, $T_{ij}^v(t)$ and $T_{ij}^w(t)$ are functions of time to be determined, and $X_i(x)$ and $Y_j(y)$ are given by

$$X_i(x) = \sum_{r=0}^{R_i} \frac{(-1)^r(2i-2r)!}{2^i r!(i-r)!(i-2r)!}(2x/L-1)^{i-2r},$$

$$Y_j(y) = \sum_{r=0}^{R_j} \frac{(-1)^r(2j-2r)!}{2^j r!(j-r)!(j-2r)!}(2y/b-1)^{j-2r}, \tag{23}$$

in which

$$R_i = \begin{cases} i/2 & \text{if } i \text{ is even}, \\ (i-1)/2 & \text{if } i \text{ is odd}. \end{cases} \tag{24}$$

Note that $X_i(x)$ and $Y_j(y)$ are the Legendre polynomials. It is also noted that $\sin(i+1)\pi x/L$ as well as $X_i(x)$ and $Y_j(y)$ are admissible functions which satisfy the essential boundary conditions. The weighting functions $\bar{u}$, $\bar{v}$ and $\bar{w}$ can be approximated with the same equations as Eq. (22) except the time-dependent functions $T_{ij}^u(t)$, $T_{ij}^v(t)$ and $T_{ij}^w(t)$. In the weighting functions, these functions should be replaced by arbitrary time-dependent functions that are represented by $\bar{T}_{ij}^u(t)$, $\bar{T}_{ij}^v(t)$ and $\bar{T}_{ij}^w(t)$.

The discretized equations of motion can be obtained by using the arbitrariness of the time-dependent functions, $\bar{T}_{ij}^u(t)$, $\bar{T}_{ij}^v(t)$ and $\bar{T}_{ij}^w(t)$, after substituting the trial and weighting functions into the weak forms. The resultant discretized equations may be represented by matrix–vector equations. The matrix-vector equations of motion can be written as

$$\mathbf{M}^{uv}\ddot{\mathbf{T}}^{uv} + 2V\mathbf{G}^{uv}\dot{\mathbf{T}}^{uv} + (V^2\mathbf{H}^{uv} + \dot{V}\mathbf{G}^{uv} + \mathbf{K}^{uv})\mathbf{T}^{uv} = \mathbf{F}^{uv}, \tag{25}$$

$$\mathbf{M}^{w}\ddot{\mathbf{T}}^{w} + 2V\mathbf{G}^{w}\dot{\mathbf{T}}^{w} + [V^{2}\mathbf{H}^{w} + \dot{V}\mathbf{G}^{w} + \mathbf{K}^{w}(\mathbf{T}^{uv})]\mathbf{T}^{w} = \mathbf{F}^{w}, \tag{26}$$

where the superposed dot stands for differentiation with respect to time, $\mathbf{T}^{uv}$ and $\mathbf{T}^{w}$ are unknown vectors given by

$$\begin{aligned}\mathbf{T}^{uv} = \{&T^{u}_{00}, T^{u}_{10}, \ldots, T^{u}_{N_x0}, T^{u}_{01}, T^{u}_{11}, \ldots, T^{u}_{N_x1}, \ldots, T^{u}_{0N_y}, T^{u}_{1N_y}, \ldots, T^{u}_{N_xN_y},\\ &T^{v}_{00}, T^{v}_{10}, \ldots, T^{v}_{N_x0}, T^{v}_{01}, T^{v}_{11}, \ldots, T^{v}_{N_x1}, \ldots, T^{v}_{0N_y}, T^{v}_{1N_y}, \ldots, T^{v}_{N_xN_y}\}^{\mathrm{T}},\\ T^{w} = \{&T^{w}_{00}, T^{w}_{10}, \ldots, T^{w}_{M_x0}, T^{w}_{01}, T^{w}_{11}, \ldots, T^{w}_{M_x1}, \ldots, T^{w}_{0M_y}, T^{w}_{1M_y}, \ldots, T^{w}_{M_xM_y}\}^{\mathrm{T}},\end{aligned} \tag{27}$$

where $\mathbf{M}^{uv}$ and $\mathbf{M}^{w}$ are the mass matrices for the in-plane and out-of-plane motions, respectively, $\mathbf{G}^{uv}$ and $\mathbf{G}^{w}$ are the matrices related to the gyroscopic force, $\mathbf{H}^{uv}$ and $\mathbf{H}^{w}$ are the matrices related to the centrifugal force, $\mathbf{K}^{uv}$ and $\mathbf{K}^{w}$ are the structural stiffness matrices, and $\mathbf{F}^{uv}$ and $\mathbf{F}^{w}$ are the applied force vectors. It should be pointed out that the out-of-plane stiffness matrix $\mathbf{K}^{w}$ is not a constant matrix but a function of the in-plane displacement vector $\mathbf{T}^{uv}$. Therefore, the in-plane matrix–vector equation of Eq. (25) is linear while the out-of-plane matrix–vector equation of Eq. (26) is nonlinear.

4. Time integration method

A solution procedure needs to be established to calculate the dynamic responses of the axially moving membrane. In this study, a computation algorithm using the generalized-α time integration method [22] is proposed to obtain dynamic responses. Before presenting the algorithm, it is necessary to define the approximate values of $\mathbf{T}^{uv}$, $\dot{\mathbf{T}}^{uv}$ and $\ddot{\mathbf{T}}^{uv}$ at time $t = t_n$ as $\mathbf{d}^{uv}_n$, $\mathbf{v}^{uv}_n$ and $\mathbf{a}^{uv}_n$, respectively. Similarly, the approximate values of $\mathbf{T}^{w}$, $\dot{\mathbf{T}}^{w}$ and $\ddot{\mathbf{T}}^{w}$ at time $t = t_n$ are denoted by $\mathbf{d}^{w}_n$, $\mathbf{v}^{w}_n$ and $\mathbf{a}^{w}_n$.

In order to compute dynamic responses of the moving membrane using the generalized-α method, it is necessary to rewrite the matrix–vector equations of Eqs. (25) and (26) as the following balance equations.

$$\mathbf{M}^{uv}\mathbf{a}^{uv}_{n+1-\alpha_m} + 2V_{n+1-\alpha_f}\mathbf{G}^{uv}\mathbf{v}^{uv}_{n+1-\alpha_f} + (V^{2}_{n+1-\alpha_f}\mathbf{H}^{uv} + \dot{V}_{n+1-\alpha_f}\mathbf{G}^{uv} + \mathbf{K}^{uv})\mathbf{d}^{uv}_{n+1-\alpha_f} = \mathbf{F}^{uv}_{n+1-\alpha_f} \tag{28}$$

$$\mathbf{M}^{w}\mathbf{a}^{w}_{n+1-\alpha_m} + 2V_{n+1-\alpha_f}\mathbf{G}^{w}\mathbf{v}^{w}_{n+1-\alpha_f} + [V^{2}_{n+1-\alpha_f}\mathbf{H}^{w} + \dot{V}_{n+1-\alpha_f}\mathbf{G}^{w} + \mathbf{K}^{w}(\mathbf{d}^{uv}_{n+1-\alpha_f})]\mathbf{d}^{w}_{n+1-\alpha_f} = \mathbf{F}^{w}_{n+1-\alpha_f}, \tag{29}$$

where the subscripts $n+1-\alpha_m$ and $n+1-\alpha_f$ represent interior interpolations between the values of time steps t_n and t_{n+1}:

$$\begin{aligned}&\mathbf{d}^{uv}_{n+1-\alpha_f} = \alpha_f\mathbf{d}^{uv}_n + (1-\alpha_f)\mathbf{d}^{uv}_{n+1}, \quad \mathbf{v}^{uv}_{n+1-\alpha_f} = \alpha_f\mathbf{v}^{uv}_n + (1-\alpha_f)\mathbf{v}^{uv}_{n+1},\\ &\mathbf{a}^{uv}_{n+1-\alpha_m} = \alpha_m\mathbf{a}^{uv}_n + (1-\alpha_m)\mathbf{a}^{uv}_{n+1}, \quad \mathbf{F}^{uv}_{n+1-\alpha_f} = \mathbf{F}^{uv}(\alpha_f t_n + (1-\alpha_f)t_{n+1}),\end{aligned} \tag{30}$$

$$\begin{aligned}&\mathbf{d}^{w}_{n+1-\alpha_f} = \alpha_f\mathbf{d}^{w}_n + (1-\alpha_f)\mathbf{d}^{w}_{n+1}, \quad \mathbf{v}^{w}_{n+1-\alpha_f} = \alpha_f\mathbf{v}^{w}_n + (1-\alpha_f)\mathbf{v}^{w}_{n+1},\\ &\mathbf{a}^{w}_{n+1-\alpha_m} = \alpha_m\mathbf{a}^{w}_n + (1-\alpha_m)\mathbf{a}^{w}_{n+1}, \quad \mathbf{F}^{w}_{n+1-\alpha_f} = \mathbf{F}^{w}(\alpha_f t_n + (1-\alpha_f)t_{n+1}),\end{aligned} \tag{31}$$

$$V_{n+1-\alpha_f} = V((1-\alpha_f)t_{n+1} + \alpha_f t_n), \quad \dot{V}_{n+1-\alpha_f} = \dot{V}((1-\alpha_f)t_{n+1} + \alpha_f t_n), \tag{32}$$

in which α_m and α_f are algorithmic parameters defined by the generalized-α method. The update equations for displacement and velocity are given by

$$\mathbf{d}^{uv}_{n+1} = \tilde{\mathbf{d}}^{uv}_n + \beta\Delta t^{2}\mathbf{a}^{uv}_{n+1}, \quad \mathbf{v}^{uv}_{n+1} = \tilde{\mathbf{v}}^{uv}_n + \gamma\Delta t\mathbf{a}^{uv}_{n+1}, \tag{33}$$

$$\mathbf{d}^{w}_{n+1} = \tilde{\mathbf{d}}^{w}_n + \beta\Delta t^{2}\mathbf{a}^{w}_{n+1}, \quad \mathbf{v}^{w}_{n+1} = \tilde{\mathbf{v}}^{w}_n + \gamma\Delta t\mathbf{a}^{w}_{n+1}, \tag{34}$$

where

$$\begin{aligned}&\tilde{\mathbf{d}}^{uv}_n = \mathbf{d}^{uv}_n + \Delta t\mathbf{v}^{uv}_n + (\tfrac{1}{2}-\beta)\Delta t^{2}\mathbf{a}^{uv}_n, \quad \tilde{\mathbf{d}}^{w}_n = \mathbf{d}^{w}_n + \Delta t\mathbf{v}^{w}_n + (\tfrac{1}{2}-\beta)\Delta t^{2}\mathbf{a}^{w}_n,\\ &\tilde{\mathbf{v}}^{uv}_n = \mathbf{v}^{uv}_n + (1-\gamma)\Delta t\mathbf{a}^{uv}_n, \quad \tilde{\mathbf{v}}^{w}_n = \mathbf{v}^{w}_n + (1-\gamma)\Delta t\mathbf{a}^{w}_n.\end{aligned} \tag{35}$$

In Eqs (33)–(35), β and γ are algorithmic parameters defined in terms of α_m and α_f, and Δt is the time step size between t_n and t_{n+1}:

$$\beta = (1-\alpha_m+\alpha_f)^2/4, \quad \gamma = 1/2-\alpha_m+\alpha_f, \quad \Delta t = t_{n+1}-t_n. \tag{36}$$

Introduction of Eq. (33) to the resultant equation obtained by substituting Eq. (30) into Eq. (28) leads to

$$\mathbf{A}_n^{uv}\mathbf{a}_{n+1}^{uv} = \mathbf{b}_n^{uv}, \tag{37}$$

where

$$\begin{aligned}
\mathbf{A}_n^{uv} &= (1-\alpha_m)\mathbf{M}^{uv} + 2(1-\alpha_f)\gamma\Delta t V_{n+1-\alpha_f}\mathbf{G}^{uv} + (1-\alpha_f)\beta\Delta t^2(V_{n+1-\alpha_f}^2\mathbf{H}^{uv} + \dot{V}_{n+1-\alpha_f}\mathbf{G}^{uv} + \mathbf{K}^{uv}),\\
\mathbf{b}_n^{uv} &= \mathbf{F}_{n+1-\alpha_f}^{uv} - \alpha_m\mathbf{M}^{uv}\mathbf{a}_n^{uv} - 2V_{n+1-\alpha_f}\mathbf{G}^{uv}[\alpha_f\mathbf{v}_n^{uv} + (1-\alpha_f)\tilde{\mathbf{v}}_n^{uv}]\\
&\quad - (V_{n+1-\alpha_f}^2\mathbf{H}^{uv} + \dot{V}_{n+1-\alpha_f}\mathbf{G}^{uv} + \mathbf{K}^{uv})[\alpha_f\mathbf{d}_n^{uv} + (1-\alpha_f)\tilde{\mathbf{d}}_n^{uv}].
\end{aligned} \tag{38}$$

Once the in-plane acceleration vector at time t_{n+1}, $\mathbf{a}_{n+1}^{uv}$, is updated from Eq. (37), the in-plane displacement and velocity vectors at time t_{n+1}, $\mathbf{d}_{n+1}^{uv}$ and $\mathbf{v}_{n+1}^{uv}$, are determined by Eq. (34). Similarly, the out-of-plane acceleration $\mathbf{a}_{n+1}^{w}$ is computed from

$$\mathbf{A}_n^{w}\mathbf{a}_{n+1}^{w} = \mathbf{b}_n^{w}, \tag{39}$$

where

$$\begin{aligned}
\mathbf{A}_n^{w} &= (1-\alpha_m)\mathbf{M}^{w} + 2(1-\alpha_f)\gamma\Delta t V_{n+1-\alpha_f}\mathbf{G}^{w} + (1-\alpha_f)\beta\Delta t^2[V_{n+1-\alpha_f}^2\mathbf{H}^{w} + \dot{V}_{n+1-\alpha_f}\mathbf{G}^{w} + \mathbf{K}^{w}(\mathbf{d}_{n+1-\alpha_f}^{uv})],\\
\mathbf{b}_n^{w} &= \mathbf{F}_{n+1-\alpha_f}^{w} - \alpha_m\mathbf{M}^{w}\mathbf{a}_n^{w} - 2V_{n+1-\alpha_f}\mathbf{G}^{w}[\alpha_f\mathbf{v}_n^{w} + (1-\alpha_f)\tilde{\mathbf{v}}_n^{w}]\\
&\quad - [V_{n+1-\alpha_f}^2\mathbf{H}^{w} + \dot{V}_{n+1-\alpha_f}\mathbf{G}^{w} + \mathbf{K}^{w}(\mathbf{d}_{n+1-\alpha_f}^{uv})][\alpha_f\mathbf{d}_n^{w} + (1-\alpha_f)\tilde{\mathbf{d}}_n^{w}].
\end{aligned} \tag{40}$$

With the known value of $\mathbf{a}_{n+1}^{w}$ from Eq. (39), the updated values of $\mathbf{d}_{n+1}^{w}$ and $\mathbf{v}_{n+1}^{w}$ can be determined from Eq. (34). It should be noted that Eq. (39) is a nonlinear equation because $\mathbf{A}_n^{w}$, namely, $\mathbf{K}^{w}$ is a function of $\mathbf{d}_n^{uv}$ and $\mathbf{d}_{n+1}^{uv}$. Although Eq. (39) is a nonlinear equation, the use of a nonlinear equation solver, e.g., the Newton–Rhapson method, is not necessary for updating the displacement, velocity and acceleration vectors. The reason is that $\mathbf{K}^{w}$ in the first equation of Eqs. (40) becomes a prescribed matrix after $\mathbf{d}_{n+1}^{uv}$ is computed.

To start the time integration procedure, initial values are required for the displacement, velocity and acceleration vectors. These initial values are determined by

$$\begin{aligned}
&\mathbf{d}_0^{uv} = \mathbf{T}^{uv}(0), \quad \mathbf{d}_0^{w} = \mathbf{T}^{w}(0), \quad \mathbf{v}_0^{uv} = \dot{\mathbf{T}}^{uv}(0), \quad \mathbf{v}_0^{w} = \dot{\mathbf{T}}^{w}(0), \quad \mathbf{F}_0^{uv} = \mathbf{F}^{uv}(0), \quad \mathbf{F}_0^{w} = \mathbf{F}^{w}(0),\\
&\mathbf{a}_0^{uv} = (\mathbf{M}^{uv})^{-1}\{\mathbf{F}_0^{uv} - 2V(0)\mathbf{G}^{uv}\mathbf{v}_0^{uv} - [V^2(0)\mathbf{H}^{uv} + \dot{V}(0)\mathbf{G}^{uv} + \mathbf{K}^{uv}]\mathbf{d}_0^{uv}\},\\
&\mathbf{a}_0^{w} = (\mathbf{M}^{w})^{-1}\{\mathbf{F}_0^{w} - 2V(0)\mathbf{G}^{w}\mathbf{v}_0^{w} - [V^2(0)\mathbf{H}^{w} + \dot{V}(0)\mathbf{G}^{w} + \mathbf{K}^{w}]\mathbf{d}_0^{w}\}
\end{aligned} \tag{41}$$

The time integration procedure for the dynamic response of the axially moving membrane is summarized in Table 1. Once the approximated values of $\mathbf{T}^{uv}$ and $\mathbf{T}^{w}$, which contain the approximated values for T_{ij}^{u}, T_{ij}^{v} and

Table 1
Time integration procedure for the dynamic response of the axially moving membrane

A. Initial calculations
1. Initialize $\mathbf{d}_0^{uv}$, $\mathbf{d}_0^{w}$, $\mathbf{v}_0^{uv}$, $\mathbf{v}_0^{w}$, $\mathbf{a}_0^{uv}$ and $\mathbf{a}_0^{w}$ by using Eq. (41).
2. Select the appropriate algorithmic parameters, α_m and α_f, and the time step size Δt.

B. For each time step ($n = 1, 2, \ldots, N$)
1. Compute the values of $\tilde{\mathbf{d}}_n^{uv}$, $\tilde{\mathbf{d}}_n^{w}$, $\tilde{\mathbf{v}}_n^{uv}$ and $\tilde{\mathbf{v}}_n^{w}$ by using Eq. (35).
2. Obtain the values of $\mathbf{a}_{n+1}^{uv}$ from Eq. (37).
3. Compute the values of $\mathbf{d}_{n+1}^{uv}$ and $\mathbf{v}_{n+1}^{uv}$ from Eq. (33).
4. Determine the value of $\mathbf{d}_{n+1-\alpha_f}^{uv}$ by using the first equation of Eq. (30).
5. Obtain the values of $\mathbf{a}_{n+1}^{w}$ from Eq. (39).
6. Compute the values of $\mathbf{d}_{n+1}^{w}$ and $\mathbf{v}_{n+1}^{w}$ from Eq. (34).
7. $n \leftarrow n+1$, go to Step B1.

T_{ij}^{w}, are computed, the longitudinal displacement u, the lateral displacement v and the transverse displacement w, are determined from Eq. (22).

5. Analysis and discussion

Before analysing and discussing the dynamic responses of the moving membrane, it is necessary to define the following dimensionless parameters:

$$\tilde{u}=\frac{u}{L},\quad \tilde{v}=\frac{v}{L},\quad \tilde{w}=\frac{w}{L},\quad \tilde{x}=\frac{x}{L},\quad \tilde{y}=\frac{y}{L},\quad \tilde{t}=\frac{t}{L}\sqrt{\frac{T_0/h}{\rho}},\quad \tilde{V}=V\sqrt{\frac{\rho}{T_0/h}}$$
$$\tilde{E}=\frac{E}{T_0/h},\quad \tilde{b}=\frac{b}{L},\quad \tilde{h}=\frac{h}{L},\quad \tilde{p}=\frac{p}{T_0/h},\quad \tilde{q}_x=\frac{q_x}{T_0},\quad \tilde{q}_y=\frac{q_y}{T_0},\quad \tilde{q}_{xy}=\frac{q_{xy}}{T_0}. \tag{42}$$

The dimensionless parameters used in all the numerical computations of this paper are given by $\tilde{E}=400$, $\tilde{b}=0.5$, $\tilde{h}=0.001$ and $v=0.3$.

5.1. Natural frequencies and critical speeds

Consider the eigenvalue problems that provide the natural frequencies of the axially moving membrane. Neglecting all transient terms from Eqs. (25) and (26), the equilibrium position vectors, $\mathbf{T}_{*}^{uv}$ and $\mathbf{T}_{*}^{w}$, for free vibrations can be determined by

$$\mathbf{T}_{*}^{uv}=(V^2\mathbf{H}^{uv}+\mathbf{K}^{uv})^{-1}\mathbf{F}^{uv},\quad \mathbf{T}_{*}^{w}=\mathbf{0}. \tag{43}$$

The linearized equations of Eqs. (25) and (26) around the equilibrium position vectors are given by

$$\mathbf{M}^{uv}\ddot{\mathbf{T}}^{uv}+2V\mathbf{G}^{uv}\dot{\mathbf{T}}^{uv}+(V^2\mathbf{H}^{uv}+\mathbf{K}^{uv})\mathbf{T}^{uv}=\mathbf{0},$$
$$\mathbf{M}^{w}\ddot{\mathbf{T}}^{w}+2V\mathbf{G}^{w}\dot{\mathbf{T}}^{w}+[V^2\mathbf{H}^{w}+\mathbf{K}^{w}(\mathbf{T}_{*}^{uv})]\mathbf{T}^{w}=\mathbf{0}, \tag{44}$$

where $\mathbf{K}^{w}(\mathbf{T}_{*}^{uv})$ is a constant matrix.

Assuming the solutions of Eq. (44) as

$$\mathbf{T}^{uv}=\mathbf{X}^{uv}\exp(\lambda_{uv}t),\quad \mathbf{T}^{w}=\mathbf{X}^{w}\exp(\lambda_{w}t), \tag{45}$$

where λ_{uv} and λ_{w} are the eigenvalues for the in-plane and out-of-plane motions, respectively, $\mathbf{X}^{uv}$ and $\mathbf{X}^{w}$ are the corresponding eigenvectors, the eigenvalue problems may be written by

$$(\lambda_{uv}^2\mathbf{M}^{uv}+2V\lambda_{uv}\mathbf{G}^{uv}+V^2\mathbf{H}^{uv}+\mathbf{K}^{uv})\mathbf{X}^{uv}=\mathbf{0},\quad [\lambda_{w}^2\mathbf{M}^{w}+2\lambda_{w}V\mathbf{G}^{w}+V^2\mathbf{H}^{w}+\mathbf{K}^{w}(\mathbf{T}_{*}^{uv})]\mathbf{X}^{w}=\mathbf{0}. \tag{46}$$

Since the natural frequencies are the imaginary parts of the eigenvalues, the dimensionless natural frequencies for the in-plane and out-of-plane motions may be written as

$$\tilde{\omega}_{uv}=\mathrm{Im}\left(\lambda_{uv}\frac{L}{\pi}\sqrt{\frac{\rho}{T_0/h}}\right),\quad \tilde{\omega}_{w}=\mathrm{Im}\left(\lambda_{w}\frac{L}{\pi}\sqrt{\frac{\rho}{T_0/h}}\right). \tag{47}$$

The convergence test provides adequate numbers of the basis function for accurate computation. The convergence characteristics of the out-of-plane natural frequencies $\tilde{\omega}_{w}$ are presented in Table 2, where the natural frequencies are computed when $\tilde{V}=0.5$. As shown in Table 2, the convergence of the out-of-plane natural frequencies is mainly dependent on M_y rather than M_x. The convergences of the in-plane natural frequencies are omitted in this paper, because they have been already discussed in Ref. [17]. For the following numerical computations, the total number of the basis functions and time step size are selected as $M_x=M_y=N_x=N_y=7$ and $\Delta\tilde{t}=0.01$.

It is interesting to compare the natural frequencies of the in-plane and out-of-plane motions. Figs. 2 and 3 show the dimensionless in-plane natural frequencies $\tilde{\omega}_{uv}$ and the out-of-plane natural frequencies $\tilde{\omega}_{w}$, respectively, for the variation of the dimensionless translating velocity $\tilde{V}$. As shown in Figs. 2 and 3, the out-of-plane natural frequencies are much less than the in-plane natural frequencies. It is well known that the critical speed is defined as the lowest speed when one of the natural frequencies becomes zero, that is, when

Table 2
Convergence characteristics of the dimensionless out-of-plane natural frequencies $\tilde{\omega}_w$ when the membrane has the dimensionless translating speed $\tilde{V} = 0.5$

M_x	M_y	Mode					
		(0, 1)	(0, 2)	(0, 3)	(1, 1)	(1, 2)	(1, 3)
3	3	0.7147	0.7320	0.7557	1.5460	1.5727	1.6446
	4	0.7147	0.6918	0.7324	1.5460	1.5249	1.6446
	5	0.6541	0.6918	0.7143	1.5054	1.5249	1.6133
	6	0.6541	0.5955	0.7143	1.5054	1.4833	1.6133
	7	0.5073	0.5955	0.6596	1.4527	1.4833	1.5687
4	3	0.7127	0.7305	0.7550	1.4562	1.4787	1.5412
	4	0.7127	0.6897	0.7313	1.4562	1.4395	1.5338
	5	0.6521	0.6897	0.7119	1.4248	1.4395	1.5080
	6	0.6521	0.5930	0.7119	1.4248	1.4081	1.5080
	7	0.5038	0.5930	0.6556	1.3845	1.4081	1.4659
5	3	0.7115	0.7294	0.7543	1.4559	1.4781	1.5391
	4	0.7115	0.6883	0.7300	1.4559	1.4389	1.5287
	5	0.6495	0.6883	0.7106	1.4233	1.4389	1.5033
	6	0.6495	0.5882	0.7106	1.4233	1.4050	1.5033
	7	0.4947	0.5882	0.6533	1.3770	1.4050	1.4613
6	3	0.7114	0.7292	0.7541	1.4466	1.4706	1.5347
	4	0.7114	0.6881	0.7299	1.4466	1.4282	1.5241
	5	0.6492	0.6881	0.7103	1.4111	1.4282	1.4976
	6	0.6492	0.5878	0.7103	1.4111	1.3908	1.4976
	7	0.4939	0.5878	0.6514	1.3602	1.3908	1.4537
7	3	0.7109	0.7289	0.7540	1.4463	1.4702	1.5346
	4	0.7109	0.6876	0.7296	1.4463	1.4280	1.5235
	5	0.6488	0.6876	0.7099	1.4111	1.4280	1.4970
	6	0.6488	0.5876	0.7099	1.4111	1.3901	1.4970
	7	0.4938	0.5876	0.6503	1.3527	1.3901	1.4527

the membrane is dynamically unstable. Comparing Figs. 2 and 3, it is observed that the dimensionless critical speed for the in-plane motion is $\tilde{V} \cong 6.96$ while the critical speed for the out-of-plane motion is $\tilde{V} \cong 0.73$. Since the critical speed for the out-of-plane motion is less than the speed for the in-plane motion, the dynamic stability is subjected to the out-of-plane critical speed.

5.2. Dynamic responses for the in-plane and out-of-plane displacements

The dynamic responses of the moving membrane are investigated when the translating velocity is prescribed. Fig. 4 illustrates ramped profiles of the dimensionless velocity, which may be expressed by

$$\tilde{V} = \begin{cases} \tilde{V}_{\max}\tilde{t}/40 & \text{for } 0 \leqslant \tilde{t} \leqslant 40, \\ \tilde{V}_{\max} & \text{for } \tilde{t} \geqslant 40, \end{cases} \tag{48}$$

where $\tilde{V}_{\max}$ is the maximum velocity of a given velocity profile. An impulsive pressure with magnitude of $\tilde{p} = 0.002$ is applied over the entire membrane surface at the initial time. Two values of $\tilde{V}_{\max}$, i.e., 0.65 and 0.75 are chosen in this paper, because the out-of-plane critical speed $\tilde{V} = 0.73$ is between these values.

The dynamic responses for the ramped velocity profiles with $\tilde{V}_{\max} = 0.65$ and $\tilde{V}_{\max} = 0.75$ are presented in Figs. 5 and 6, respectively. The displacements are computed at a point defined by $\tilde{x} = 0.5$ and $\tilde{y} = 0.125$. Note that $\tilde{V}_{\max} = 0.65$ is less than the critical speeds for both the in-plane and out-of-plane motions. Therefore, when the translating velocity changes according to the ramped profile with $\tilde{V}_{\max} = 0.65$, the dynamic responses for the in-plane displacements, $\tilde{u}$ and $\tilde{v}$, as well as the out-of-plane displacement, $\tilde{w}$, are bounded and stable, as shown in Fig. 5. However, when $\tilde{V}_{\max} = 0.75$ or when the maximum translating speed is larger than

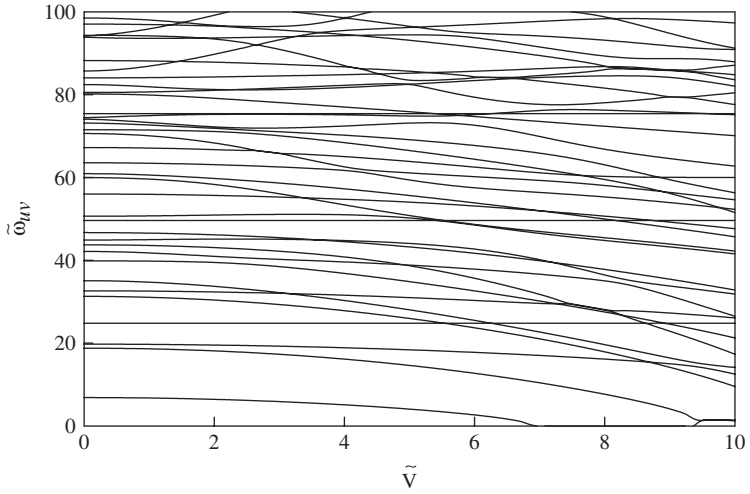

Fig. 2. Dimensionless natural frequencies of the in-plane motion for the variation of the dimensionless translating velocity.

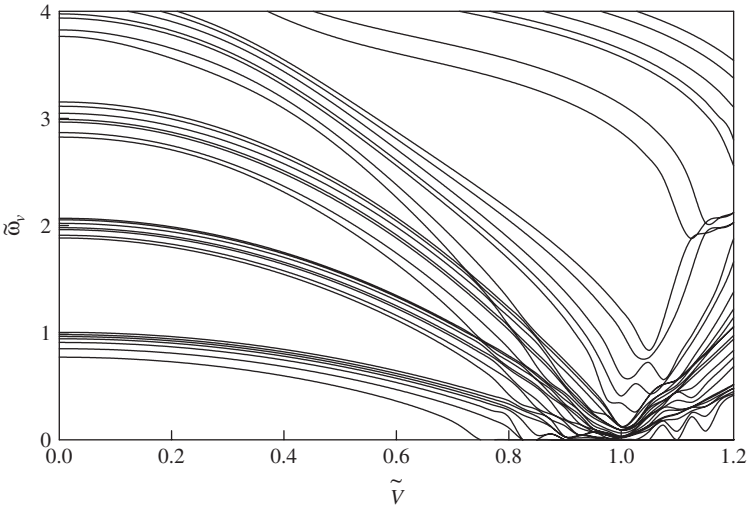

Fig. 3. Dimensionless natural frequencies of the out-of-plane motion for the variation of the dimensionless translating velocity.

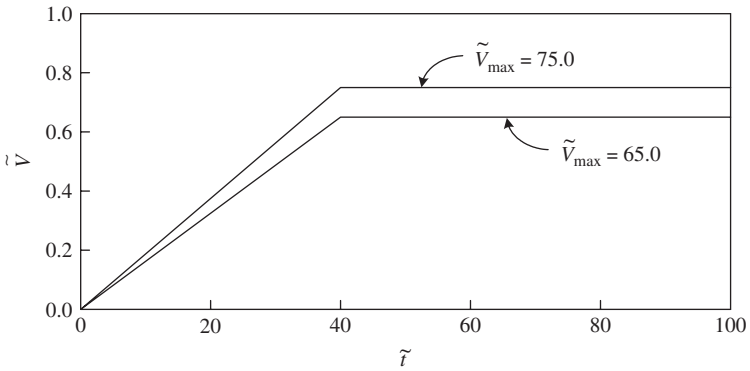

Fig. 4. Ramped profiles of the dimensionless velocity.

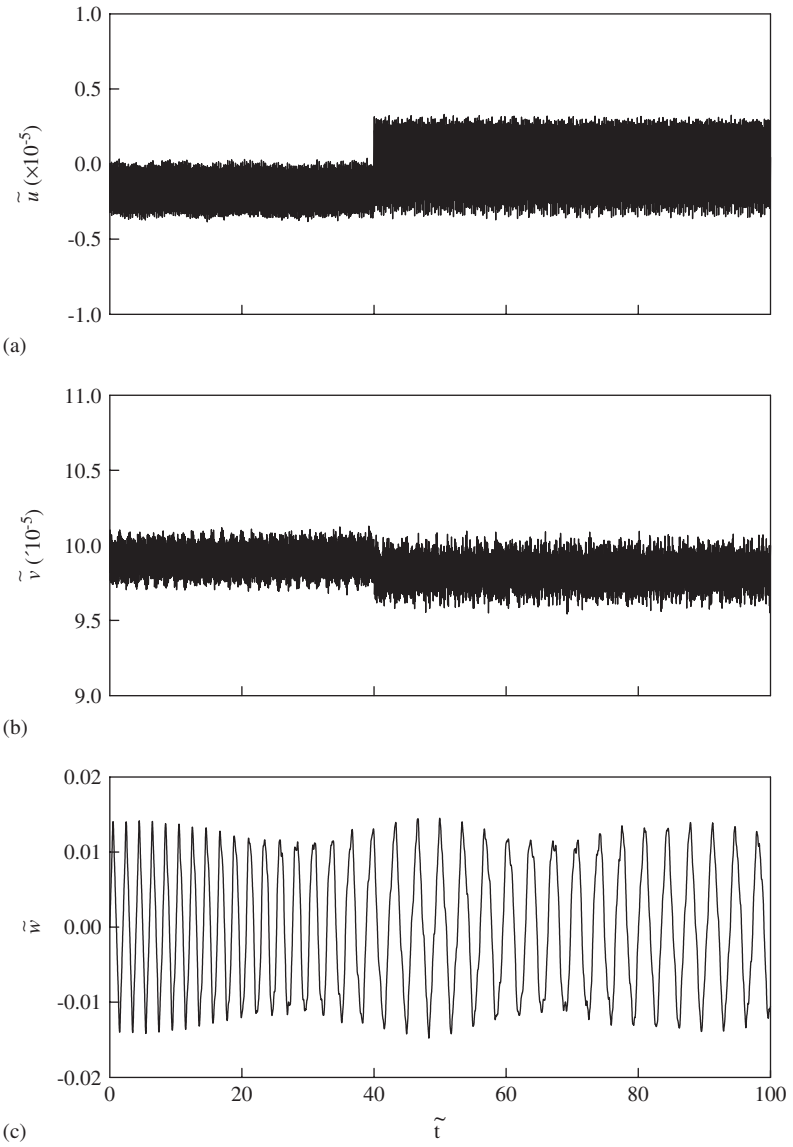

Fig. 5. Dynamic responses of the dimensionless displacements when the translating velocity has the ramped profile with $\tilde{V}_{\max} = 0.65$: (a) the longitudinal displacement $\tilde{u}$, (b) the lateral displacement $\tilde{v}$, and (c) the transverse displacement $\tilde{w}$.

the out-of-plane critical speed and less than the in-plane critical speed, $\tilde{u}$ and $\tilde{v}$ are bounded but $\tilde{w}$ becomes unbounded, as illustrated in Fig. 6.

It is interesting to compare the dynamic responses between the in-plane and out-of-plane displacements. Figs. 5 and 6 show that the in-plane responses have shorter periods than the out-of-plane response. This is an expected result because the in-plane natural frequencies are larger than the out-of-plane frequencies, as shown in Figs. 2 and 3. An amplitude modulation, which is often called the beat phenomenon, is observed in Fig. 5(c). This modulation is caused by a bundle of the natural frequencies with very close values, shown in Fig. 3.

The effects of the translating acceleration on the dynamic responses need to be analysed. Since the slope of a velocity profile in Fig. 4 represents the translating acceleration, the dimensionless acceleration corresponding to the ramped profile given by Eq. (48) is $\tilde{V}_{\max}/40$ for $0 \leqslant \tilde{t} \leqslant 40$ and zero for $\tilde{t} \geqslant 40$. Figs. 5(a) and 6(a) show that the longitudinal displacements $\tilde{u}$ have a zero average value when the accelerations are zero, i.e., $\tilde{t} \geqslant 40$, while they have negative average values when the accelerations are positive, i.e., $0 \leqslant \tilde{t} \leqslant 40$. This results from

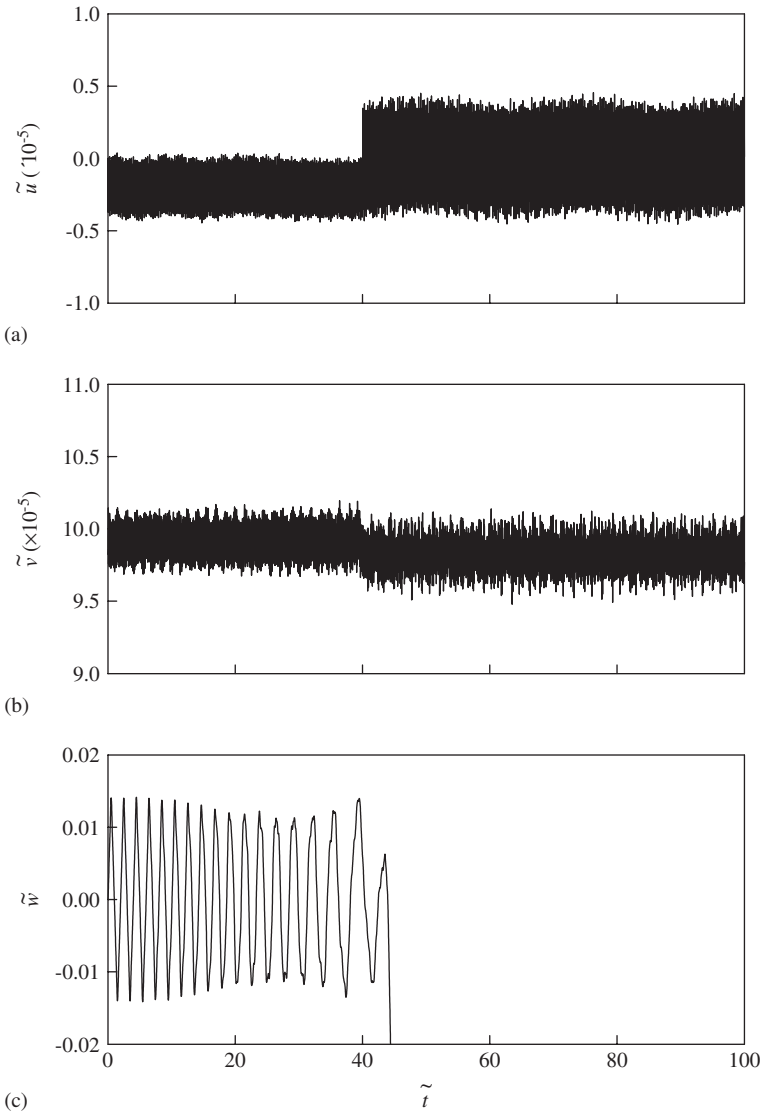

Fig. 6. Dynamic responses of the dimensionless displacements when the translating velocity has the ramped profile with $\tilde{V}_{\max} = 0.75$: (a) the longitudinal displacement $\tilde{u}$, (b) the lateral displacement $\tilde{v}$, and (c) the transverse displacement $\tilde{w}$.

the inertia effect due to the positive acceleration. A similar phenomenon is observed in the lateral displacements $\tilde{v}$ which are described in Figs. 5(b) and 6(b). The effects of the accelerations on $\tilde{w}$ can be seen in $0 \leqslant \tilde{t} \leqslant 40$ of Figs. 5(c) and 6(c), where it is found that the periods of the transverse vibration increase with time. This phenomenon happens because the natural frequencies decrease due to the positive accelerations.

The effects of translating velocity profiles are also investigated. A smooth velocity profile of Fig. 7 is considered for comparison, which can be expressed as

$$\tilde{V} = \begin{cases} \tilde{V}_{\max}\tilde{t}/40 - (\tilde{V}_{\max}\tilde{t}/40)\sin(\pi\tilde{t}/20) & \text{for } 0 \leqslant \tilde{t} \leqslant 40, \\ \tilde{V}_{\max} & \text{for } \tilde{t} \geqslant 40, \end{cases} \tag{49}$$

where $\tilde{V}_{\max} = 0.65$. With this profile, the dynamic responses computed at a point given by $\tilde{x} = 0.5$ and $\tilde{y} = 0.125$ are presented in Fig. 8. Comparing the responses of the smooth and ramped profiles, prominent differences are observed in the responses for $\tilde{u}$ and $\tilde{v}$; however, no apparent difference is observed in the

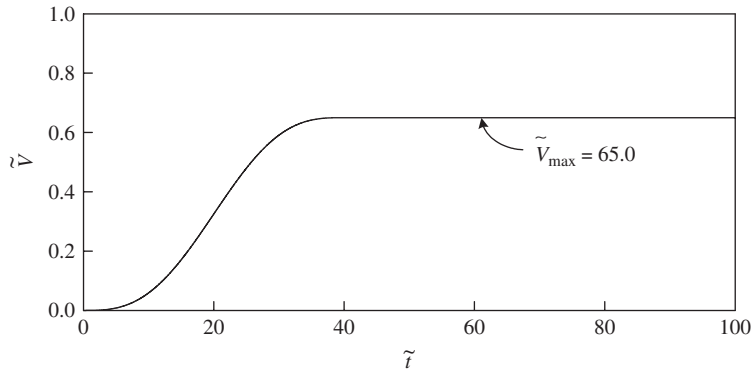

Fig. 7. Smooth profile of the dimensionless velocity.

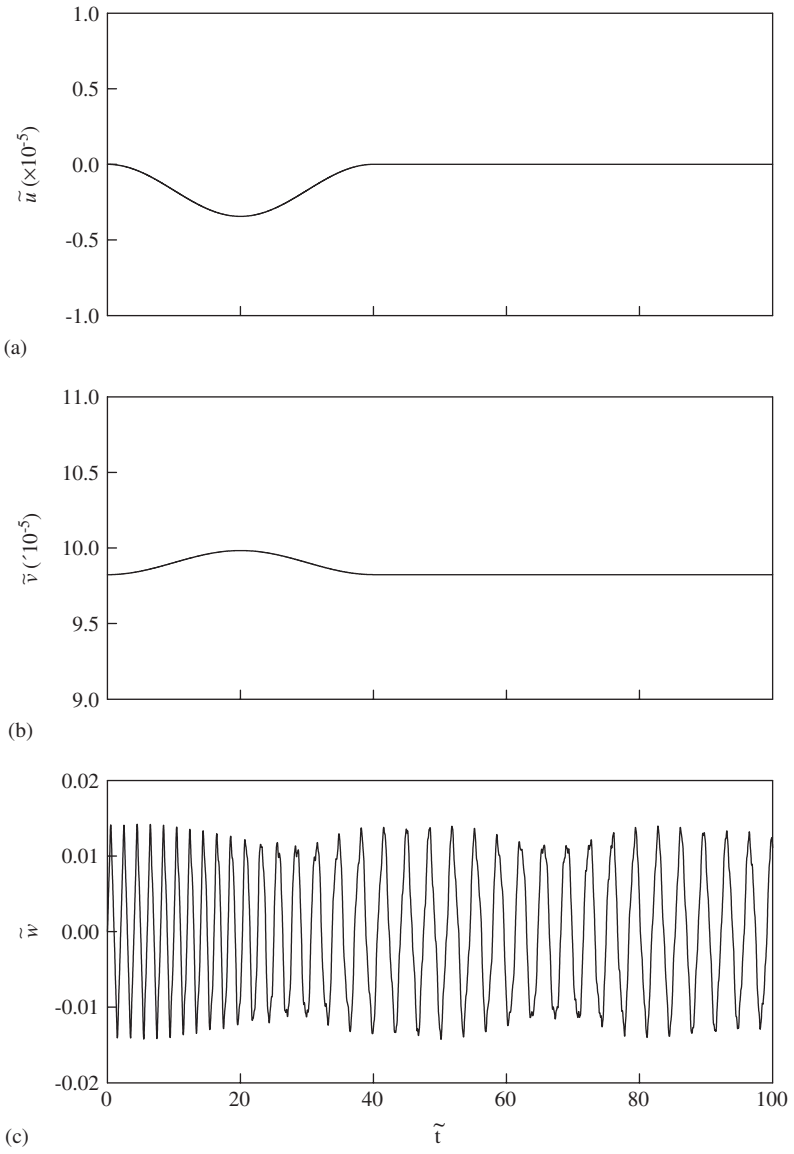

Fig. 8. Dynamic responses of the dimensionless displacements when the translating velocity has the smooth profile with $\tilde{V}_{max} = 0.65$: (a) the longitudinal displacement $\tilde{u}$, (b) the lateral displacement $\tilde{v}$, and (c) the transverse displacement $\tilde{w}$.

responses of $\tilde{w}$. When $\tilde{t} = 0$ or 40, the ramped profile possesses suddenly changed acceleration, but the smooth profile dose not. The acceleration without a sudden change yields vibration-free responses for $\tilde{u}$ and $\tilde{v}$, as shown in Fig. 8(a) and (b).

5.3. Deformed shapes and stress distributions

It is valuable to investigate the deformed shapes and stress distributions of the moving membrane. The deformed shapes and the stress distributions are computed at given time $\tilde{t} = 60$ when the translating velocity is prescribed by the ramped profile with $\tilde{V}_{\max} = 0.65$, as expressed by Eq. (48). The deformed shape due to the in-plane displacements $\tilde{u}$ and $\tilde{v}$ is illustrated in Fig. 9 and the deformed shape due to the out-of-plane displacement $\tilde{w}$ is illustrated in Fig. 10. As shown in Fig. 9, the in-plane deformed shape is symmetric with respect to the centrelines of the membrane parallel to the x and y axes. It is seen that the middle part is shrunk in the y direction except the end parts. This deformed shape results from the x-directional tension and the no-slip conditions at the rollers. Since the impulsive pressure is applied over the entire surface of the membrane, the out-of-plane displacement of the membrane has a bulging shape at the central part, as depicted in Fig. 10. This implies that the central part may have the largest magnitude of vibration.

When the translating velocity has the ramped profile with $\tilde{V}_{\max} = 0.65$, the stress distributions at $\tilde{t} = 60$ are shown in Fig. 11, where Figs. 11(a)–(c) are for the dimensionless membrane forces, $\tilde{q}_x$, $\tilde{q}_y$ and $\tilde{q}_{xy}$, respectively. As shown in Fig. 11(a), the x-directional normal stress $\tilde{q}_x$ has a larger value at the middle part corresponding to $y = b/2$, compared to the top and bottom parts. On the other hand, it is observed from Fig. 11(b) that both end parts defined by $x = 0$ and L have relatively larger $\tilde{q}_y$ than other parts. The dimensionless shear stress $\tilde{q}_{xy}$, presented in Fig. 11(c), demonstrates that the four corner of the membrane have relatively larger values of the shear stress. From the stress distributions, it may be inferred that the moving membrane may be broken

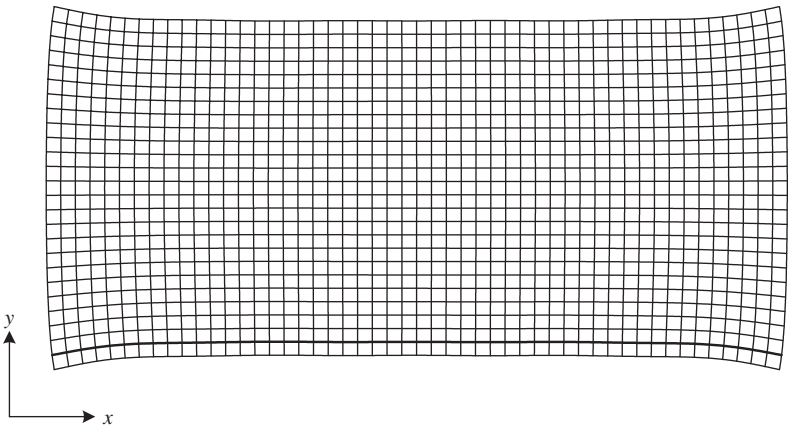

Fig. 9. Deformed shape due to the in-plane displacements $\tilde{u}$ and $\tilde{v}$ when $\tilde{t} = 60$ and $\tilde{V} = 0.65$.

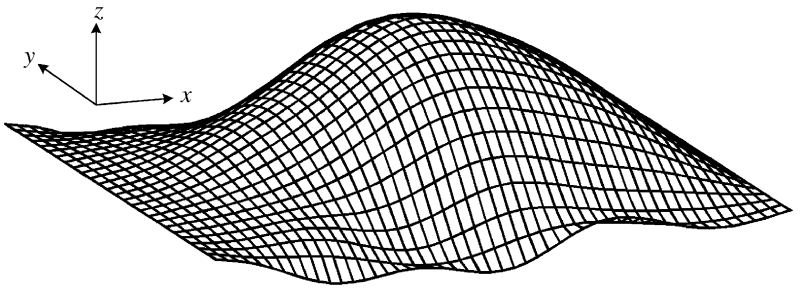

Fig. 10. Deformed shape due to the out-of-plane displacement $\tilde{w}$ when $\tilde{t} = 60$ and $\tilde{V} = 0.65$.

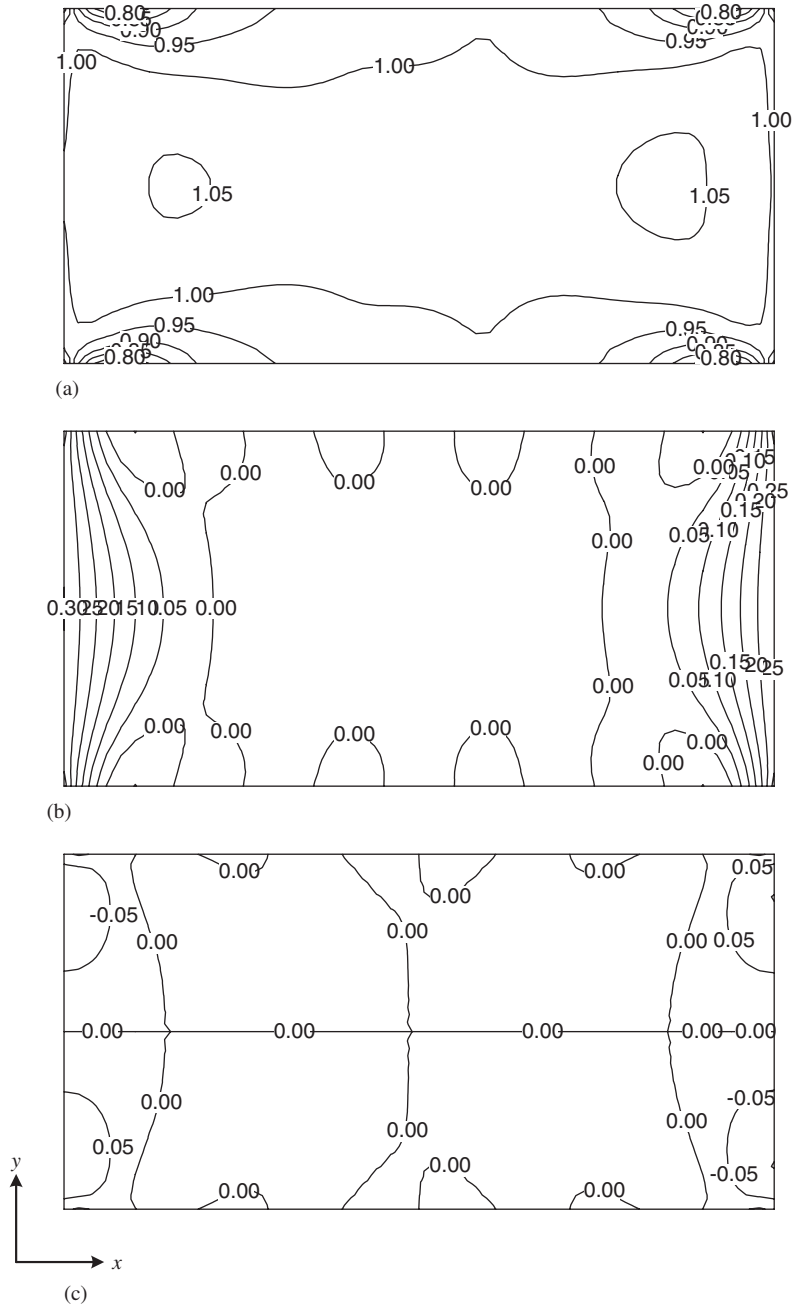

Fig. 11. Stress distributions when $\tilde{t} = 60$ and $\tilde{V} = 0.65$: (a) $\tilde{q}_x$, (b) $\tilde{q}_y$, and (c) $\tilde{q}_{xy}$.

around the rollers if it has a severe vibration. The reason is that the parts in the neighbourhood of the rollers have high stress concentration.

6. Summary and conclusions

The dynamic responses for the axially moving membrane are investigated in this paper. Considering the geometric nonlinearity, the equations of motion are derived with the no-slip boundary conditions at the rollers. The derived equations consist of linear and nonlinear equations for the in-plane and out-of-plane

motion, respectively. These equations are transformed to the weak forms, which are discretized by applying the Galerkin method. In order to obtain dynamic responses, a method which does not use a nonlinear equation solver is presented.

It is observed that the in-plane responses have shorter periods than the out-of-plane response because the former has higher natural frequencies than the latter. It is also found that dynamic instability occurs in the out-of-plane motion rather than in the in-plane motion because the out-of-plane motion has a lower critical speed than the in-plane motion. The out-of-plane responses exhibit the increasing period with the translating velocity and the amplitude modulation due to close natural frequencies. Prominent differences between the smooth and ramped profiles can be found not in out-of-plane motion but in the in-plane motion. Finally, the central region of the membrane has relatively large displacements and the regions near the rollers have high stress concentrations.

Acknowledgement

This work was supported by Korea Research Foundation Grant (KRF-2004-041-D00043).

References

[1] J.A. Wickert, C.D. Mote Jr., Classical vibration analysis of axially moving continua, *ASME Journal of Applied Mechanics* 57 (1990) 738–744.
[2] J.A. Wickert, C.D. Mote Jr., Traveling load response of an axially moving string, *Journal of Sound and Vibration* 149 (1991) 267–284.
[3] R.G. Parker, Supercritical speed stability of the trivial equilibrium of an axially moving string on an elastic foundation, *Journal of Sound and Vibration* 221 (1999) 205–219.
[4] J.S. Chen, Natural frequencies and stability of an axially traveling string in contact with a stationary load system, *ASME Journal of Vibration and Acoustics* 119 (1997) 152–157.
[5] J.A. Wickert, C.D. Mote Jr., Response and discretization methods for axially moving materials, *ASME Applied Mechanics Reviews* 44 (1991) 279–284.
[6] K.Y. Lee, A.A. Renshaw, Solution of the moving mass problem using complex eigenfunction expansions, *ASME Journal of Applied Mechanics* 67 (2000) 823–827.
[7] R.K. Jha, R.G. Parker, Spatial discretization of axially moving media vibration problems, *ASME Journal of Vibration and Acoustics* 122 (2000) 290–294.
[8] L. Zhang, J.W. Zu, Nonlinear vibrations of viscoelastic moving belts—part I: free vibration analysis, *Journal of Sound and Vibration* 216 (1998) 75–91.
[9] L. Zhang, J.W. Zu, Nonlinear vibrations of viscoelastic moving belts—part II: forced vibration analysis, *Journal of Sound and Vibration* 216 (1998) 93–105.
[10] F. Pellicano, F. Vestroni, Nonlinear dynamics and bifurcations of an axially moving beam, *ASME Journal of Vibration and Acoustics* 122 (2000) 21–30.
[11] L. Meirovitch, A new method of solution of the eigenvalue problem for gyroscopic systems, *AIAA Journal* 12 (1974) 1337–1342.
[12] G.M.T. D'Eleuterio, P.C. Huges, Dynamics of gyroelastic continua, *ASME Journal of Applied Mechanics* 51 (1984) 415–422.
[13] M. Pakdemirli, A.G. Ulsoy, Stability analysis of an axially accelerating string, *Journal of Sound and Vibration* 203 (1997) 815–832.
[14] L. Zhang, J.W. Zu, Nonlinear vibration of parametrically excited moving belts—part I: dynamic response, *ASME Journal of Applied Mechanics* 66 (1999) 396–402.
[15] L. Zhang, J.W. Zu, Nonlinear vibration of parametrically excited viscoelastic moving belts—part II: stability analysis, *ASME Journal of Applied Mechanics* 66 (1999) 403–409.
[16] J.A. Wickert, Analysis of self-excited longitudinal vibration of a moving tape, *Journal of Sound and Vibration* 160 (1993) 455–465.
[17] C. Shin, W. Kim, J. Chung, Free in-plane vibration of an axially moving membrane, *Journal of Sound and Vibration* 272 (2004) 137–154.
[18] H. Koivurova, A. Pramila, Nonlinear vibration of axially moving membrane by finite element method, *Computational Mechanics* 20 (1997) 573–581.
[19] J. Niemi, A. Pramila, FEM-analysis of transverse vibrations of an axially moving membrane immersed in ideal fluid, *International Journal for Numerical Methods in Engineering* 24 (1987) 2301–2313.
[20] X. Wang, Finite element analysis of air-sheet interactions and flutter suppression devices, *Computers and Structures* 64 (1997) 983–994.
[21] D.B. McIver, Hamilton's principle for systems of changing mass, *Journal of Engineering Mathematics* 7 (1972) 249–261.
[22] J. Chung, G.M. Hulbert, A time integration algorithm for structural dynamics with improved numerical dissipation: the generalized-α method, *Journal of Applied Mechanics* 60 (1993) 371–375.